Magnetization measurements on Li2Pd3B superconductor

doi: 10.1063/1.1814433

Magnetization measurements on Li_2Pd_3B superconductor

P. Badica[a)]
Institute for Materials Research, Tohoku University, 2-1-1 Katahira, Aoba-ku, Sendai, 980-8577, Japan and National Institute for Materials Physics, P.O. Box MG-7, 76900 Bucharest, Romania

T. Kondo, T. Kudo, Y. Nakamori, S. Orimo, and K. Togano
Institute for Materials Research, Tohoku University, 2-1-1 Katahira, Aoba-ku, Sendai, 980-8577, Japan

(Received 17 March 2004; accepted 7 September 2004)

Magnetization in *dc* magnetic fields and at different temperatures has been measured on the antiperovskite Li_2Pd_3B with a cubic structure composed of distorted Pd_6B octahedrons. This material was recently found to exhibit superconductivity at 7–8 K. The critical fields $H_{c1}(0)$ and $H_{c2}(0)$ are determined to be 135 Oe and 4 T, respectively. Critical current density, scaling of the pinning force within the Kramer model, and irreversibility field data are presented. Several superconductivity parameters were deduced: Coherence length $\xi=9.1$ nm, penetration depth $\lambda=194$ nm, and Ginzburg–Landau parameter $\kappa=21$. The material resembles other boride superconductors from the investigated points of view. © *2004 American Institute of Physics*. [DOI: 10.1063/1.1814433]

We have recently found superconductivity below 7–8 K in the cubic Li_2Pd_3B compound.[1] The material is a boride and the constituent elements are an alkaline element, Li and a late transition element, Pd. None of these elements have been reported to be included in the binary or ternary boride superconductors as base ones, although the alkaline earth, Mg, is a component of MgB_2 with the surprising high T_c of 39 K, and Pd belongs to the platinum group of elements that are usually included in the boride superconductors (Ru, Rh, Os, Ir, and Pt).[2] Also of interest is that Pd is a base element of the boride carbide compound Y–Pd–B–C showing the maximum T_c of 23 K (Ref. 3) in this class of superconductors.

In this letter, we present the magnetization measurements performed by a superconducting quantum interference device magnetometer (Quantum Design 5T) with the purpose of extracting the data on critical fields, critical current, and superconductivity parameters. Evaluation of Li_2Pd_3B against other superconductors is important for the generation of directions in the search for superconductors, e.g., targeting higher T_c, as well as for a better understanding of superconductivity. The idea is that this compound has a cubic antiperovskite structure[4] composed of distorted Pd_6B octahedrons centered by boron. It resembles metal oxide superconductors, such as the high-T_c ones, ruthenates, bismuthates, and sodium cobaltates, in which metal atoms are surrounded by oxygen in an octahedral arrangement. Li_2Pd_3B is also interesting from another point of view. This material is another example of a perovskite nonoxide superconductor containing octahedral units, such as $MgNi_3C$ (Ref. 5) ($T_c=7.6$ K), but while the structure of $MgNi_3C$ is very symmetrical, in Li_2Pd_3B a distorted structure is present. According to Sardar and Sa,[6] from the theoretical point of view, this distortion might be important for the occurrence and/or control of superconductivity, i.e., this intrinsic distortion can produce self-doping of the material toward the formation of superconductivity or modification of the critical temperature T_c, in a similar manner as in high-temperature superconductor (HTS) when a nonintrinsic pressure (external pressure or chemical pressure) is applied.

Material was synthesized by arc melting employing a two-step procedure: First, ingots of Pd_3B alloy were prepared, and second, they were melted together with the Li metal. The resulting material is the Li_2Pd_3B superconductor. Details on processing, T_c, and the structure of the as-prepared superconductor are given elsewhere.[1]

Magnetization loops $M(H)$ taken at different temperatures are presented in Fig. 1, while the magnetization curves versus temperature $M(T)$, measured for several magnetic fields, are presented in Fig. 2. Upper critical field (H_{c2}^{M-H}) was determined as the point where the $M(H)$ loops reach the background [Fig. 1 inset (a)]. Upper critical field (H_{c2}^{M-T}) was also estimated considering the onset point of the superconducting transition of the $M(T)$ curves (Fig. 2). Variation of H_{c2}^{M-H} and H_{c2}^{M-T}, as a function of temperature, is shown in Fig. 3. From the linear fitting of the experimental points, at

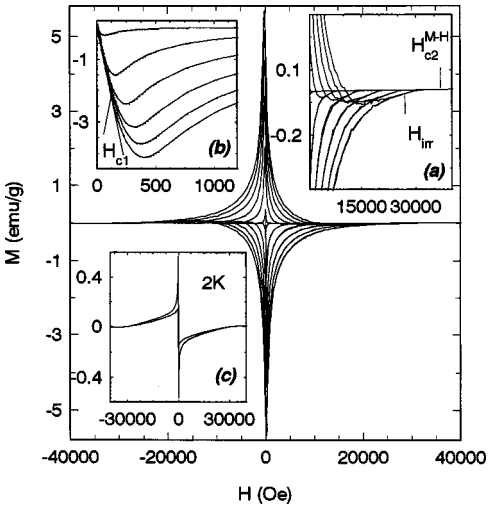

FIG. 1. Magnetization loops $M(H)$ at 2, 3, 4, 5, 6, and 7 K for the Li_2Pd_3B bulk sample. Insets (a) and (b) show details of the same curves at high and low magnetic fields, respectively. Inset (c) shows a $M(H)$ loop at 2 K for the sample in the powdered state.

[a)]Electronic mail: p.badica@imr.tohoku.ac.jp

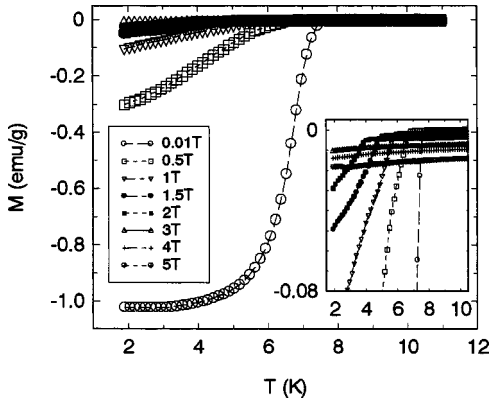

FIG. 2. Magnetization curves vs temperature for different applied magnetic fields. The inset gives detail showing the variation in the onset of the diamagnetic signal.

$T=0$ K, H_{c2}^{M-H} and H_{c2}^{M-T} are 5 T and 5.2 T, respectively [Fig. 3]. These values are comparable with the 6.2 T value determined from measurements of electrical resistance in magnetic fields.[1] In the following calculations, we have used the intermediate curve, i.e., that for H_{c2}^{M-T}. In this case, the absolute value of the initial slope dH_{c2}/dT is 0.7 T/K and is not far from the value 0.8 T/K for the Pd-containing boride–carbide Y–Pd–B–C.[7] Assuming the Werthamer–Hefland–Hohemberg formula $H_{c2}(0)=0.691\times(dH_{c2}/dT)_{T_c}x\ T_c$,[8] we obtain an upper critical field $H_{c2}(0)$ of approximately 4 T. From the upper critical field ($H_{c2}=\Phi/2\pi\xi^2$, where Φ is the flux quantum) we have extracted the coherence length, $\xi=9.1$ nm. This value is similar to MgB_2,[2] it is in the upper limit of the ξ-interval for the boride carbides ($\xi\approx 6$ nm),[7] it is almost double that of $MgNi_3C$ ($\xi=4.6$ nm)[9,10] and is considerably larger than the values estimated for HTS cuprates (typically 2 nm).

Another important parameter characterizing superconductivity is the lower critical field H_{c1}. Values of H_{c1} were taken as the field for which the $M(H)$ curve starts to deviate from the linear behavior generated by perfect diamagnetism [Fig. 1 inset (b)]. Data are plotted versus temperature in the inset of Fig. 3. Fitting with $H_{c1}=H_{c1}(0)[1-(T/T_c)^2]$ results in $H_{c1}(0)=135$ Oe and $T_c=7.5$ K. The value of T_c from fitting agrees relatively well with the experimental value of 7.8 K. The value of $H_{c1}(0)$ is considerably lower than for the boride–carbide superconductors (around 800 Oe)[7] with high T_c, is comparable to values measured for $MgNi_3C$ (100 Oe)[10] and is also approximately two to three times

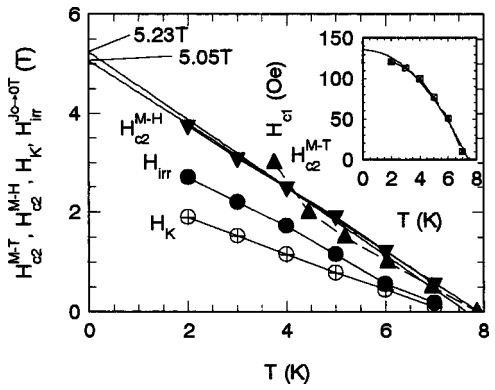

FIG. 3. Critical fields vs temperature.

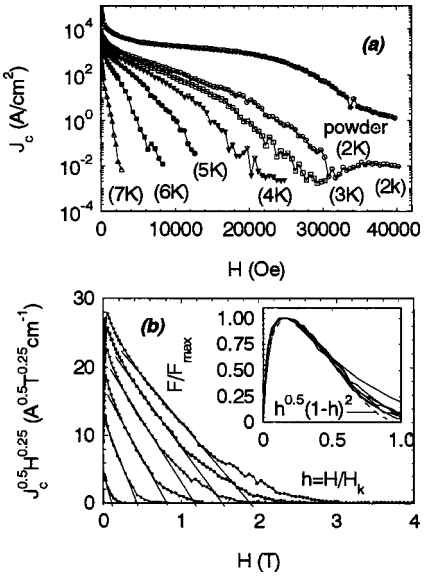

FIG. 4. Critical current density vs applied magnetic field (a) for the Li_2Pd_3B sample in the powder and bulk states and Kramer curves (b) for different temperatures of 2, 3, 4, 5, 6, and 7 K (the curve for the highest temperature is closer to the left low corner of the plot). The inset presents the scaling of the pinning force. The dashed line is the fitting with $h^{0.5}(1-h)^2$.

lower than for MgB_2,[2] but is slightly higher than for the Re–boride superconductors (60–80 Oe).[11] From $H_{c1}(0)$ and ξ, the penetration depth can be calculated to be $\lambda=194$ nm, by the formula $H_{c1}=(\Phi_0/4\pi\lambda^2)\ln(\lambda/\xi)$. This value is similar to the high limit of the λ-interval for MgB_2 (Ref. 2) and is comparable to λ for $MgNi_3C$ ($\lambda=248$ nm).[10] The Ginzburg–Landau parameter $\kappa=\lambda/\xi=21$. The extracted value is between the values reported for boride superconductors Re_7B_3 (Ref. 11) with hexagonal structure ($\kappa=17$) and Re_3B (Ref. 11) with orthorhombic structure ($\kappa=35$), and is approximately two times lower than for $MgNi_3C$ ($\kappa=54$).[10]

Critical current density, J_c, versus magnetic field was evaluated using Bean model[12] ($J_c=30\Delta M/d$, where d is the diameter of the bulk sample in our case) is presented in Fig. 4(a). The values of J_c are relatively low (e.g., $J_c(0\text{ T},2\text{ K})=5\times10^3$ A/cm^2). The reason seems to be the presence of cracks. To check this assumption, we measured a $M(H,2K)$ loop on part of the bulk sample after it was crushed into powder [Fig. 1 inset (c)]. The resulting powder as well as the surface of the initial sample, showing cracks, can be seen in Fig. 5. The curve of J_c for the powder sample, considering the average grain size $d=20$ μm in the Bean model, is plotted in Fig. 4(a). The value of $J_c(0\text{ T},2\text{ K})$ is 6×10^4 A/cm^2 for the powder sample. An optical microscopy image on the polished cross section of the bulk sample[1] indicates that the domains between the cracks are approximately five to ten times smaller than the size of the sample. Therefore, if, in the Bean model, calculation is done by using the size of these domains, the values of $J_c(0\text{ T})$ will be close to those observed for the powder sample. This suggests that the observed discrepancy in the values of J_c is not due to the "weak links" problem as it is for high-T_c superconductors.

Moreover, the Kramer curves $J_c^{0.5}H^{0.25}(H)$ (Ref. 13) from Fig. 4(b) are approximately linear in H and are similar to Nb_3Sn (Ref. 14) and MgB_2,[15] considered without weak links. Scaling with the classic $h^{0.5}(1-h)^2$ function of the flux pinning force, $F_p=J_c\mu_0H$, is found within the whole measured

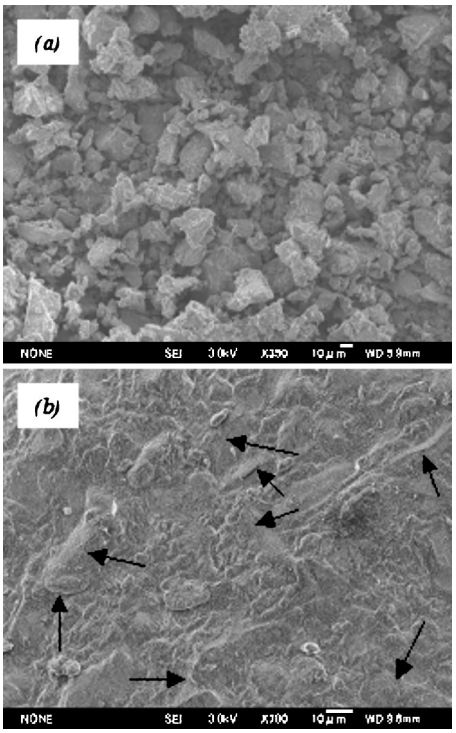

FIG. 5. SEM (JEOL JSM 6700) images of the Li_2Pd_3B sample in the (a) powder and (b) bulk state. On image (b), the cracks are indicated by the arrows.

interval of 2–7 K [Fig. 4(b) inset]. Extrapolation of the relatively linear region of the Kramer curves results in $H_k(T)$-field values equivalent to the empirical irreversibility line for which J_c tends to zero. This imperfect linearity of the Kramer curves suggests the possibility of effects, or of effects not specific to conventional boride superconductors. This idea is of interest since unconventional behavior in the J_c (transport) of $MgNi_3C$, also having no weak links, was recently reported.[16] Data of $H_k(T)$ together with the experimental $H_{irr}(T)$ extracted from the $M(H)$ loops for the same criterion of $J_c \rightarrow 0$ [Fig. 1 inset (a)] are presented in Fig. 3. Both $H_k(T)$ and $H_{irr}(T)$ curves are linear, but they do not overlap, probably due to the forced fitting of the relatively linear region in the Kramer curves, as well as due to the difficulties (noted by many authors) in determination of the H_{irr} point for which $J_c \rightarrow 0$. Despite this discrepancy, both lines are directly proportional to $H_{c2}(T)$. This result is similar to MgB_2 (Ref. 15) and is very different from the $(T_c - T)^{1.5}$ dependence observed for the $H_{irr}(T)$ in HTS.[17] Possible reasons for the difference in behavior of the H_{irr} in classic superconductors and HTS are discussed in the review article.[17]

In summary, we have characterized Li_2Pd_3B compound using magnetization measurements. The material is shown to be a classic intermetallic boride superconductor from the investigated points of view. On the other hand, the lack of weak links, as in the classic superconductors and structural features similar to HTS, increases expectations of identification of directions in the search for superconductors with improved characteristics. Li_2Pd_3B might be especially important because, together with $MgNi_3C$, it can be viewed as a bridge between HTS and conventional intermetallic superconductors. However, more experiments are necessary in order to establish the nature of the superconductivity in Li_2Pd_3B.

The authors thank E. Aoyagi and Y. Hayasaka of Tohoku University for help with scanning electron microscopy (SEM) measurements, and K. Hirata of NIMS and L. Miu of INCDFM for useful discussions.

[1] K. Togano, P. Badica, Y. Nakamori, S. Orimo, H. Takeya, and K. Hirata, cond-mat/0402232.
[2] C. Buzea and T. Yamashita, Supercond. Sci. Technol. **14**, R115 (2001).
[3] R. J. Cava, H. Takagi, B. Batlogg, H. W. Zandbergen, J. J. Krajewski, W. F. Peck, R. B. Vandover, R. J. Felder, T. Siegrist, K. Mizuhashi, J. O. Lee, H. Eisaki, S. A. Carter, and S. Uchida, Nature (London) **367**, 146 (1994).
[4] U. Eibenstein and W. Jung, J. Solid State Chem. **133**, 21 (1997).
[5] T. He, Q. Huang, A. P. Ramirez, Y. Wang, K. A. Regan, N. Rogado, M. A. Hayward, M. K. Haas, J. S. Slusky, K. Inumara, H. W. Zandbergen, N. P. Ong, and R. J. Cava, Nature (London) **411**, 54 (2001).
[6] M. Sardar and D. Sa, Physica C **411**, 120 (2004).
[7] H. Takagi, R. J. Cava, H. Eisaki, J. O. Lee, K. Mizuhashi, B. Batlogg, S. Uchida, J. J. Krajewski, and W. F. Peck, Physica C **228**, 389 (1994).
[8] N. Werthamer, E. Hefland, and P. C. Hohenberg, Phys. Rev. **147**, 295 (1966).
[9] S. Y. Li, R. Fan, X. H. Chen, C. H. Wang, W. Q. Mo, K. Q. Ruan, Y. M. Xiong, X. G. Luo, H. T. Zhang, L. Li, Z. Sun, and L. Z. Cao, Phys. Rev. B **64**, 132505 (2001).
[10] Z. Q. Mao, M. M. Rosario, K. D. Nelson, K. Wu, I. G. Deac, P. Schiffer, Y. Liu, T. He, A. Regan, and R. J. Cava, Phys. Rev. B **67**, 094502 (2003).
[11] A. Kawano, Y. Mizuta, H. Takagiwa, T. Muranaka, and J. Akimitsu, J. Phys. Soc. Jpn. **72**, 1724 (2003).
[12] C. P. Bean, Phys. Rev. Lett. **8**, 250 (1962).
[13] E. J. Kramer, J. Appl. Phys. **44**, 1360 (1973).
[14] D. Dew-Hughes, Philos. Mag. B **55**, 459 (1987).
[15] D. C. Larbalestier, L. D. Cooley, M. O. Rikel, A. A. Polyanskii, J. Jiang, S. Patnaik, S. Y. Cai, D. M. Feldmann, A. Gurevich, A. A. Squitieri, M. T. Naus, C. B. Eom, E. E. Hellstrom, R. J. Cava, K. A. Regan, N. Rogado, M. A. Hayward, T. He, J. S. Slusky, P. Khalifah, K. Inumaru, and M. Haas, Nature (London) **410**, 186 (2001).
[16] D. P. Young, M. Moldovan, and P. W. Adams, cond-mat/0312651.
[17] Y. Yeshurun, A. P. Molozemoff, and A. Shaulov, Rev. Mod. Phys. **68**, 911 (1996).